JOURNAL OF VIROLOGY, Jan. 2003, p. 1268–1280 Vol. 77, No. 2
0022-538X/03/$08.00+0 DOI: 10.1128/JVI.77.2.1268–1280.2003

Microarray Analysis of Host Cell Gene Transcription in Response to Varicella-Zoster Virus Infection of Human T Cells and Fibroblasts In Vitro and SCIDhu Skin Xenografts In Vivo

Jeremy O. Jones* and Ann M. Arvin

Departments of Pediatrics and Microbiology and Immunology, Stanford University, Stanford, California

Received 19 August 2002/Accepted 17 October 2002

During primary infection, varicella-zoster virus (VZV) is spread via lymphocytes to skin, where it induces a rash and establishes latency in sensory ganglia. A live, attenuated varicella vaccine (vOka) was generated by using the VZV Oka strain (pOka), but the molecular basis for vOka attenuation remains unknown. Little is known concerning the effects of wild-type or attenuated VZV on cellular gene regulation in the host cells that are critical for pathogenesis. In this study, transcriptional profiles of primary human T cells and fibroblasts infected with VZV in cell culture were determined by using 40,000-spot human cDNA microarrays. Cellular gene transcription in human skin xenografts in SCID mice that were infected with VZV in vivo was also evaluated. The profiles of cellular gene transcripts that were induced or inhibited in infected human foreskin fibroblasts (HFFs), T cells, and skin in response to pOka and vOka infection were similar. However, significant alterations in cellular gene regulation were observed among the three differentiated human cell types that were examined, suggesting specific differences in the biological consequences of VZV infection related to the target cell. Changes in cellular gene transcription detected by microarray analysis were confirmed for selected genes by quantitative real-time reverse transcription-PCR analysis of VZV-infected cells. Interestingly, the transcription of caspase 8 was found to be decreased in infected T cells but not in HFFs or skin, which may signify a tissue-specific antiapoptosis mechanism. The use of microarrays to demonstrate differences in effects on host cell genes in primary, biologically relevant cell types provides background information for experiments to link these various response phenotypes with mechanisms of VZV pathogenesis that are important for the natural course of human infection.

Varicella-zoster virus (VZV) is the etiological agent of two common diseases: varicella (chicken pox) and herpes zoster (shingles). VZV is the smallest of the alphaherpesviruses, with a genome consisting of approximately 125 kbp that contains at least 70 unique open reading frames (ORFs) and three duplicated genes, ORFs 62 and 71, 63 and 70, and 64 and 69 (22). The VZV DNA genome is packaged in an icosahedral capsid surrounded by the tegument, comprising viral proteins that initiate DNA replication when the virus enters the host cell, and a lipid membrane envelope containing the viral glycoproteins that are presumed to mediate cell entry. As is characteristic of herpesviruses, VZV replication depends on the expression of immediate-early regulatory genes, of which that encoding the IE62 gene product is predominant, early genes, including those encoding viral kinases, and late genes, such as that encoding the essential glycoprotein, gE (12).

The pathogenesis of primary VZV infection involves mucosal inoculation of infectious particles, followed by a lymphocytic cell-associated viremia with spread to distant sites, including skin and neural tissue, before effective VZV-specific immunity is induced (8). Primary VZV infection induces both innate and antigen-specific immune responses. The innate response, including natural killer cell activation and interferon production, probably limits the initial spread of VZV, but adaptive immunity is responsible for recovery from varicella and zoster as well as for preserving VZV latency (6). A live attenuated varicella vaccine (vOka) was created by multiple passages of a wild-type parent Oka (pOka) strain in guinea pig embryo cells and human fibroblasts (26). Subcutaneous inoculation of vOka does not cause illness in most children, indicating that viremia does not occur or is subclinical, yet it elicits adaptive immunity (4, 6). While vOka is attenuated in healthy children, it remains infectious in some immunocompromised children and can cause zoster (29).

Very little is known about the effects of wild-type VZV or vOka infection on host cells at the molecular level. Like other viruses, VZV is assumed to obstruct certain host cell processes and co-opts the machinery and resources of the cell to make viral gene products. Among its known consequences, VZV decreases cell surface expression of major histocompatibility complex class I (MHC-I) molecules in T cells and fibroblasts by causing their retention in the Golgi complex (2). VZV also interferes with the Jak/Stat signal transduction pathway, inhibiting cell surface expression of MHC-II in response to gamma interferon (1). Sequencing the pOka and vOka genomes indicates variations in many of the ORFs, some of which are predicted to alter viral proteins, precluding a simple genetic explanation for the attenuation of vOka (5, 14, 15). The virulence of vOka in human skin xenografts in SCID mouse skin is diminished, as shown by a reduced yield of infectious virus, decreased viral protein synthesis, failure to invade the dermis, and slower destruction of epidermal cells compared to pOka (19). However, infectivity for $CD4^+$ and $CD8^+$ T cells in thy-

* Corresponding author. Mailing address: 300 Pasteur Dr., Rm. G312, Stanford University School of Medicine, Stanford, CA 94305-5208. Phone: (650) 725-6555. Fax: (650) 725-8040. E-mail: jjones@stanford.edu.

mus and liver implants is intact, and vOka retains the capacity to decrease the cell surface expression of MHC-I molecules on infected T cells (2).

Microarrays, in which mRNA transcription patterns can be determined for many thousands of genes simultaneously, have emerged as a new method for evaluating virus-host cell interactions (10, 11, 13, 17, 20, 27). In this study, we explored the transcriptional changes in cellular genes after VZV infection of human T cells and fibroblasts in vitro and human skin xenografts in SCIDhu mice in vivo. Using human cDNA microarrays and the Statistical Analysis for Microarrays (SAM) program (29), we defined transcriptional profiles following VZV infection of these cell types with pOka and vOka. Our objectives were (i) to characterize the effects of VZV on human T-cell gene transcription, since cell-associated viremia is an essential step in the pathogenesis of primary VZV infection, (ii) to evaluate whether microarrays could be used to assess effects on host cell genes after VZV infection of skin in xenografts in vivo, (iii) to identify any similarities in up-regulation or down-regulation of cell gene transcription related to VZV infection in T cells, fibroblasts, and skin, and (iv) to determine whether any differences in responses to pOka and the clinically attenuated vOka virus could be identified in any of the target cell types.

MATERIALS AND METHODS

Viruses and cells. The viruses were recombinant pOka and vOka, derived from pOka cosmids made from pOka DNA (6 passages) or vOka cosmids made from vOka DNA (11 passages in human embryonic lung cells, 6 in guinea pig embryo cells, and further passage in HEL cells); the viruses were transferred from infected melanoma cells to human foreskin fibroblasts (HFFs) (16, 25). HFFs were grown in T150 flasks in Dulbecco's modified Eagle's medium supplemented with 10% fetal bovine serum, 2 mM L-glutamine, 50 U of penicillin/ml, and 50 μg of streptomycin/ml at 37°C. Cells were harvested 2 to 4 days after VZV inoculation, when ~85% of cells exhibited cytopathic changes. At this time point, infected cells express all classes of viral genes, including immediate-early, early, and late genes (8, 12). Primary human T cells were obtained from fresh pediatric tonsil specimens according to a protocol approved by the Stanford University Committee for the Protection of Human Subjects in Research. Briefly, tonsillar tissue was disrupted mechanically in media, and cells were filtered and passed through a nylon wool column to deplete B cells; T cells were purified by Ficoll-Paque gradient separation followed by negative magnetic selection (Stem Cell Technologies, Vancouver, British Columbia, Canada) to remove cells expressing CD14, CD16, CD19, CD56, and glycophorin A. T cells were suspended in RPMI medium, and equal numbers (5×10^6 to 5.0×10^7) were overlaid on VZV-infected or uninfected HFF monolayers. After 48 h, nonadherent cells were resuspended in media and subjected to a Ficoll-Paque gradient to recover T cells and remove dead cells and fibroblasts. This time point was selected based on experiments showing that transfer of VZV from infected fibroblasts to T cells is optimal at 48 h (30). An aliquot of each T-cell suspension was tested for surface expression of late VZV proteins by flow cytometry using phycoerythrin-labeled CD3 and high-titer human anti-VZV immunoglobulin G (IgG) (18). Each array in which T cells were the source of RNA used T cells from a single donor; tonsillar T cells were not pooled. Human skin implants in SCID mice were infected with VZV and harvested at 21 or 28 days after infection, as described previously; infectious virus was recovered from all implants, as determined by an infectious-focus assay (18).

Microarrays. Total RNA was isolated from infected and uninfected HFFs and T cells by double extraction with Trizol-chloroform (Gibco-BRL) and phenol-chloroform-isoamyl alcohol, precipitated in isopropanol, and resuspended in diethyl pyrocarbonate-treated water. Skin implants were homogenized (Tissue Tearor; Biospec, Inc.) before RNA extraction. RNA (25 μg/specimen) was used to create a cDNA probe. Briefly, RNA was denatured for 10 min at 65°C in the presence of an oligo(dT) primer (Invitrogen, Inc.) and reverse transcribed for 2 h at 42°C with SuperScript II (Gibco-BRL) in the presence 25 mM dATP, dCTP, and dGTP; 10 mM dTTP; and 1 mM Cy3- (uninfected-cell RNA) or Cy5 (infected-cell RNA)-labeled dUTP (Amersham, Inc.). The RNA was degraded, and the remaining cDNA was washed three times in Tris-EDTA (TE) buffer and purified in a Centricon-30 microconcentrator (Amicon, Inc.). In the last wash, the cDNA was blocked with 20 μg each of Cot-1 human DNA (Gibco-BRL, Inc.), poly(A) RNA (Sigma, Inc.), and tRNA (Gibco-BRL, Inc.) to remove non-mRNA. The cDNA was resuspended in 32 μl of TE, and 1.05 μl of 10% sodium dodecyl sulfate and 5.95 μl of 20× SSC (1× SSC is 0.15 M NaCl plus 0.015 M sodium citrate) were added. This mixture was denatured by heating for 2 min at 100°C, incubated at room temperature for 20 min, and centrifuged for 10 min. The 31,000- to 42,000-spot human cDNA microarrays were those developed by Patrick Brown (23), Department of Biochemistry, Stanford University (http://genome-www4.Stanford.EDU/cgi-bin/sfgf/home.pl). The cDNA probe was added to a microarray slide, covered with a 22- by 60-mm LifterSlip (Erie Scientific, Portsmouth, N.H.), and hybridized at 65°C for 14 to 16 h. Prior to hybridization, arrays were postprocessed according to the Brown laboratory protocol (http://cmgm.stanford.edu/pbrown/protocols/index.html). The arrays were scanned with a Gene Pix Scanner 4000A (Axon Instruments, Inc.) and analyzed with the Scanalyze program (Eisen, shareware, http://rana.lbl.gov/).

Microarray data analysis. Data were entered into the Stanford Microarray Database (SMD) for normalization, filtering, and retrieval (24). The standard SMD normalization was selected for all arrays. The quality of the arrays was determined by three highly restrictive parameters, including a computed normalization close to 1, an appropriate data distribution, and consistent staining over the entire microarray. By these criteria, seven T-cell arrays (three pOka and four vOka), four HFF arrays (two pOka and two vOka), and seven skin arrays (three pOka and four vOka) were selected for analysis. The log (base 2) of the R/G normalized ratio (mean) was selected as the data to be retrieved for analysis. The data-filtering criteria required that spots, which correspond to arrayed genes, not be flagged and have a regression correlation value of >0.6, that each channel (e.g., color) for a spot have a intensity/background ratio of >1.5, that spots have a $\log_2$ of the R/G normalized ratio (mean) greater than 1 standard deviation from the mean, and that spots have an absolute value greater than 1.0 in at least two (HFFs) or three (T cells) arrays. To be included in the data analysis, a gene was required to meet these criteria on >70% of the arrays for each cell type, that is, on three out of the four HFF arrays or five out of seven T-cell or skin arrays.

The SAM program was used to analyze the data after downloading into Excel (28). Briefly, SAM computes a statistic, d_i, for each gene i measuring the strength of the relationship between gene expression and the response variable. It uses repeated permutations to determine if the expression of any gene is significantly related to the response. The program creates a profile of observed versus expected values, and values which lie outside a user-defined region of this profile are considered significantly related to the response, or in this case, significantly regulated genes. One-class response analyses were conducted to identify significant changes in gene regulation compared to a control in a particular cell type. Two-class response analyses were conducted to assess variance between microarray data generated in separate experiments with the same cell type, which provided a further stringent test of the quality of the microarray data. Two-class response analyses were also used to identify significant differences between transcriptional profiles induced by pOka and vOka and to compare effects of VZV infection on cellular genes in the three different cell types that were examined. All of the raw data and the SAM analysis plots can be viewed at http://cmgm.stanford.edu/~jjones. The raw data can also be found on the SMD at http://genome-www5.stanford.edu/MicroArray/SMD.

Quantitative real-time RT-PCR. Primers were designed to amplify highly conserved 250-bp regions of the caspase 8, MX2, ADAR, and β-globin mRNA transcripts. RNA was extracted from infected and uninfected cells by a double Trizol-chloroform treatment and precipitated in isopropanol. Reverse transcription-PCR (RT-PCR), quantification, and melting curve analysis were performed on an iCycler iQ machine (Bio-Rad, Inc.). For each primer pair, a standard curve was established to quantify the experimental samples. Total RNA, 250 ng, diluted in 10 ng of yeast tRNA/ml, was reverse transcribed and amplified with the EZ r*Tth* RNA PCR kit (Applied Biosystems, Inc.) in the presence of 1× SYBR Green (1:10,000 dilution of Molecular Probes stock) and 1× fluorescein (dilution of stock). The cycling conditions were as follows: 60 min at 60°C for RT; 2 min at 95°C, 30 s at 95°C, and 2 min at 68°C repeated 40 times; and then a 50-step melting curve analysis wherein the annealing temperature was decreased by 0.5°C during each step. Each experimental sample was compared to the standard curve generated from the same plate in order to determine the original starting amount of a particular transcript and to a melting curve to ensure the production of a specific product. Only those samples that could be measured against a standard curve with a high correlation coefficient and a slope that implied an efficient reaction (calculated by the iCycler software) were used. Results from the multiple experiments were averaged.

Immunoblotting. Expression of gp96 (tumor rejection antigen 1; grp94) was assessed by immunoblotting T cells. Protein was harvested from pelleted cells in extract buffer (10 mM Tris, 150 mM NaCl, 10 mM NaN_3, 0.5% Triton, 0.1% NP-40), and equal amounts were loaded onto precast gradient polyacrylamide gels. The protein was transferred to a nylon membrane, blocked (5% milk in 1× phosphate-buffered saline [PBS]) for 1 h, and then probed with rat anti-grp94 (Stressgen, Inc.) at 1:500 for 1 h and washed (1× PBS, 0.1% Tween). A secondary goat anti-rat IgG-horseradish peroxidase-conjugated antibody was added at 1:1,000 for 20 min, the protein was washed, and the signal was detected with the ECL detection kit (Amersham, Inc.).

RESULTS

Statistical analysis of microarray data. Following strict selection of spots according to the defined criteria, a microarray data set was created for each cell type. Each data set was analyzed by SAM to identify changes in gene transcription related to VZV infection and to minimize other causes of transcriptional variation under the experimental conditions used for infecting each cell type. Analysis of microarray data with the SAM program has been shown to be more accurate than calculation of fold change, as determined by Northern blot confirmation of mRNA transcript changes in tumor tissue (29). The SAM software not only predicts significantly regulated genes but also predicts the number of false positives, defined as those genes that are likely to be identified incorrectly by the microarray as being regulated significantly. One of the benefits of SAM is that it provides a sliding parameter delta (represented as dashed lines in Fig. 1), the outcome of which is to vary the ratio of true positives to predicted false positives. For the purposes of these experiments, a delta parameter that yielded a high ratio of true positives to false positives was chosen for each data set. The ratios were 381:4 for T-cell arrays, 90:1 for HFF arrays, and 139:3 for skin arrays. The program also allows the user to input a threshold value at which the regulation of a gene is considered significant. As the $\log_2$ of R/G normalized ratio was the data analyzed in this study, a threshold of 1.00 was chosen, as this value corresponds to a twofold change in regulation.

A SAM one-class response analysis assumes that each array in the data set is equivalent and then determines significant differences in regulation compared to a control. In these experiments, each VZV-infected cell type was compared to the corresponding uninfected-cell type as the control. One-class analyses were performed for each data set obtained using each target cell type to create preliminary lists of significantly regulated genes. The SAM one-class response data plot for each cell type data set fit an approximately sigmoidal curve centered at 0 as illustrated for the T-cell data set (Fig. 1); each plot shows the calculated number of significant and predicted falsely significant genes (upper left corner), as well as the delta parameter and threshold values (upper right corner) used for each set. The one-class response plots of HFF and skin microarray data sets were similar to the T-cell plot, indicating that genes were both induced and inhibited in each cell type (see http://cmgm.stanford.edu/~jjones or http://genome-www5.stanford.edu/MicroArray/SMD).

In a SAM two-class response analysis, significant differences between two microarray data sets are determined. Multiple two-class response analyses were used to assess the variance among the microarrays from repeated experiments with each cell type. For this purpose, the microarray datasets were distributed into two classes in every possible combination and subjected to analysis using the same delta parameter values as those used for the one-class analyses. This control is necessary because a change in the delta parameter in SAM will change the number of positive hits; it is important to keep the parameters for defining a significantly regulated gene the same as those that were used to generate the original list of significantly regulated genes. Most two-class response analyses of the same cell type showed no differences in regulated genes; the comparison with the most variability indicated significant differences in the regulation of 22 genes (http://cmgm.stanford.edu/~jjones). Any genes that exhibited variance in these two class comparisons were eliminated from the final list of significantly regulated genes for the particular cell type. In some cases, values of replicate spots are listed separately on the final lists. The fact that the values of these replicate spots are nearly identical indicates the precision of the results across the microarrays.

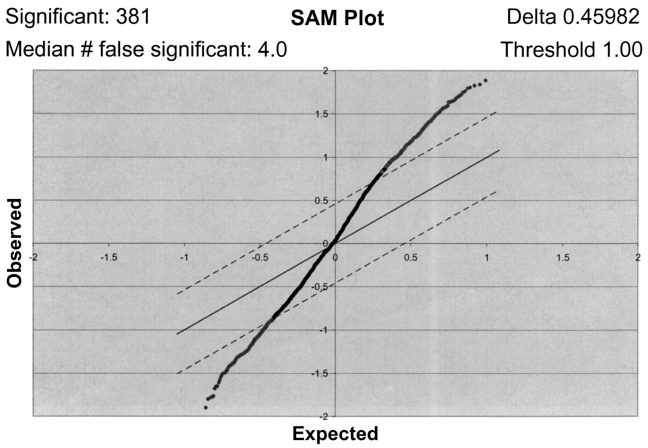

FIG. 1. One-class analysis of the T-cell microarray data set. The seven T-cell arrays were subjected to a SAM one-class analysis where the software created a field of observed versus expected gene regulation values from the array data. Threshold and delta parameter values (upper right corner) were chosen to limit the field and calculate significantly and falsely significantly regulated genes (upper left corner). The threshold value was set at 1.00, corresponding to a twofold difference in regulation from the uninfected control. Dashed lines, delta parameter, which defines the significance field; dots above the upper line, probable significantly up-regulated genes; dots below the lower line, probable significantly down-regulated genes.

Comparison of host cell transcription profiles after infection with pOka and vOka. Two-class SAM analyses were used to compare data sets for each cell type infected with pOka versus vOka. In each of these two-class analyses, the value of the delta parameter was identical to that which was used in the corresponding one-class analysis. No significant differences in gene regulation between pOka and vOka in any cell type were observed (see website). This statistical documentation of the similarity in host cell response validated the grouping of the pOka and vOka data for the one-class response analyses that were used to create lists of significantly regulated genes in particular cell types (Tables 1 and 2). That no significant differences between pOka and vOka were found was expected because the growth kinetics of pOka and vOka in HFFs and T cells in vitro are indistinguishable. Furthermore, while vOka

TABLE 1. Significantly regulated genes in VZV-infected human T cells and fibroblasts

Gene or protein[a]	SAM score	Fold change
T cells		
Immune and stress response		
MX2 (myxovirus [influenza virus] resistance 2, homolog of murine)	1.83	2.36
CAT (catalase)	1.82	3.23
STIP1 (stress-induced phosphoprotein 1; Hsp70/Hsp90-organizing protein)	1.69	2.78
CTRP2 (complement-c1q tumor necrosis factor-related protein)	1.44	2.29
FCER1G (Fc fragment of IgE, high-affinity I receptor for gamma polypeptide)	1.40	2.21
ADAR (RNA specific)	1.39	2.04
FCGR2A (Fc fragment of IgG, low-affinity IIa receptor for CD32)	1.35	2.43
CD38 antigen (p45)	1.34	2.39
MARCO (macrophage receptor with collagenous structure)	1.33	2.23
C1S (complement component 1, s subcomponent)	1.33	2.32
DYT1 (dystonia 1, torsion [autosomally dominant; torsin A])	1.19	2.33
CYP24 (cytochrome P450, subfamily XXIV [vitamin D24 hydroxylase])	1.16	2.19
TRA1 (tumor rejection antigen (gp96) 1)	1.08	2.13
FGB (fibrinogen, B beta polypeptide)	1.04	2.01
IL-17B (interleukin-17B)	1.02	2.04
SERPINH2 (serine [or cysteine] proteinase inhibitor, clade H [heat shock protein 47], member 2)	0.91	2.07
CD68 antigen	−1.52	−2.36
MIG2 (mitogen inducible 2)	−1.39	−2.21
MICA (MHC-I polypeptide-related sequence A)	−1.39	−2.85
HSPC182 protein	−1.25	−3.08
KLRC2 (killer cell lectin-like receptor subfamily C, member 2)	−1.18	−2.36
ISG20 (interferon-stimulated gene product [20 kDa])	−0.91	−2.09
Cell adhesion and structure		
COL6A2 (collagen, type VI, alpha 2)	2.08	3.46
TUBA2 (tubulin, alpha 2)	1.52	2.72
FLOT1 (flotillin 1)	1.46	2.39
CMAR (cell matrix adhesion regulator)	1.41	2.56
TNNI1 (troponin I, skeletal, slow)	1.38	2.33
CLP (coactosin-like protein)	1.29	2.15
HEF1 (enhancer of filamentation 1 [cas-like docking; Crk-associated substrate related])	1.26	2.05
LOC51143 (dynein light chain A)	1.25	2.20
TM6SF2 (transmembrane 6 superfamily member 2)	1.22	2.23
KNS2 (kinesin 2; 60–70 kDa)	1.15	2.01
ADD2 (adducin 2 [beta])	1.03	2.03
ITGA3 (integrin, alpha 3 [antigen CD49C, alpha 3 subunit of VLA-3 receptor])	0.99	2.15
LOC58498 (myosin light chain 2a)	−2.41	−2.60
SPTA1 (spectrin, alpha, erythrocytic 1 [elliptocytosis 2])	−1.45	−2.37
MYL3 (myosin, light polypeptide 3, alkali; ventricular, skeletal, slow)	−1.40	−2.85
Signal transduction: receptors, kinases/phosphatases, G proteins		
CNR1 (cannabinoid receptor 1 [brain])	1.64	2.85
NTRK2 (neurotrophic tyrosine kinase, receptor, type 2)	1.64	2.49
GUCA1A (guanylate cyclase activator 1A [retina])	1.50	3.09
CENTB5 (centaurin, beta 5)	1.43	2.54
POMZP3 (POM [POM121 rat homolog] and ZP3 fusion)	1.41	2.38
SH3BGRL3 (SH3 domain binding glutamic acid-rich protein-like 3)	1.29	2.21
PIK4CB (phosphatidylinositol 4-kinase, catalytic, beta polypeptide)	1.26	2.29
TRIP8 (thyroid hormone receptor interactor 8)	1.17	2.14
MAPK8IP2 (mitogen-activated protein kinase 8-interacting protein 2)	1.15	2.03
GKAP42 (protein kinase anchoring protein)	1.12	2.09
SYK (spleen tyrosine kinase)	1.02	2.02
TRIP11 (thyroid hormone receptor interactor 11)	−1.58	−2.93
S100A11 (S100 calcium-binding protein A11 [calgizzarin])	−1.55	−2.56
RAB3A (member of RAS oncogene family)	−1.40	−2.64
PAK4 (p21 [CDKN1A]-activated kinase 4)	−1.35	−2.24
PORIMIN (pro-oncosis receptor inducing membrane injury)	−1.33	−2.22
PTPN14 (protein tyrosine phosphatase, nonreceptor type 14)	−1.28	−2.06
GRIN2D (glutamate receptor, ionotropic, *N*-methyl D-aspartate 2D)	−1.26	−2.11
TRAF4 (TNF receptor-associated factor 4)	−1.24	−2.12
ADRA1B (adrenergic, alpha-1B-, receptor)	−1.23	−2.23
TRAF3 (TNF receptor-associated factor 3)	−1.17	−2.01
DUSP4 (Dual-specificity phosphatase 4)	−1.17	−2.85
MKP-7 (MAPK phosphatase-7)	−1.05	−2.49

Continued on following page

TABLE 1—*Continued*

Gene or protein[a]	SAM score	Fold change
Replication, transcription, translation, degradation machinery, protein modification		
RNMT (RNA [guanine-7-] methyltransferase)	1.54	2.90
SERPINB1 (serine [or cysteine] proteinase inhibitor, clade B [ovalbumin], member 1)	1.51	2.51
Cystatin C (amyloid angiopathy and cerebral hemorrhage)	1.47	2.63
MRPL9 (mitochondrial ribosomal protein L9)	1.44	2.30
TAF13 (TAF13 RNA polymerase II, TATA box binding protein-associated factor, 18 kDa)	1.38	2.23
SERPINB3 (serine [or cysteine] proteinase inhibitor, clade B [ovalbumin], member 3)	1.23	2.28
EIF4G3 (eukaryotic translation initiation factor 4 gamma, 3)	1.15	2.10
SENP3 (sentrin/SUMO-specific protease 3)	1.08	2.00
PSMB8 (proteasome [prosome, macropain] subunit, beta type, 8 [large multifunctional protease 7])	1.02	2.20
BAZ2B (bromodomain adjacent to zinc finger domain, 2B)	1.02	2.20
ARFRP1 (ADP-ribosylation factor-related protein 1)	0.89	2.09
PSMB3 (proteasome [prosome, macropain] subunit, beta)	−1.49	−3.48
RBX1 (ring-box 1)	−1.41	−2.41
CAPN3 (calpain 3, p94)	−1.33	−2.44
SERPINA3 (serine [or cysteine] proteinase inhibitor, clade A [alpha-1 antiproteinase, antitrypsin], member 3)	−1.32	−2.31
LOC51005 (CGI-14 protein)	−1.31	−2.49
U3-55K (U3 snoRNP-associated 55-kDa protein)	−1.29	−2.15
UQCRC2 (ubiquinol-cytochrome *c* reductase core protein II)	−1.29	−2.59
TAF2 (TAF2 RNA polymerase II, TATA box binding protein-associated factor, 150 kDa)	−1.26	−2.42
4E-T (eIF4E-transporter)	−1.23	−2.43
CSTF3 (cleavage stimulation factor, 3′ pre-RNA, subunit 3)	−1.13	−2.12
CBX3 (chromobox homolog 3 [Drosophila HP1 gamma])	−1.12	−2.06
ERCC1 (excision repair cross-complementing rodent repair deficiency, complementation group 1)	−1.09	−2.04
HDAC2 (histone deacetylase 2)	−1.09	−2.01
SFRS6 (splicing factor, arginine/serine-rich 6)	−1.07	−2.39
PSME3 (proteasome [prosome, macropain] activator subunit 3 [PA28 gamma; Ki])	−1.03	−2.06
PB1 polybromo 1	−0.98	−2.03
Cell cycle, development, apoptosis, transcription factors		
TMPO (thymopoietin)	1.89	3.38
CDK5R1 (cyclin-dependent kinase 5, regulatory subunit 1)	1.65	2.75
CSPG6 (chondroitin sulfate proteoglycan 6 [bamacan])	1.65	2.86
PA2G4 (proliferation-associated 2G4, 38 kDa)	1.57	2.49
IFRD1 (interferon-related developmental regulator 1)	1.56	2.32
CNNM2 (cyclin M2)	1.32	2.24
ZNF14 (zinc finger protein 14 [KOX 6])	1.25	2.01
PDGFB (platelet-derived growth factor beta polypeptide [simian sarcoma viral {v-sis} oncogene homolog])	1.22	2.08
IRLB (c-myc promoter-binding protein)	1.16	2.20
IFRD1 (interferon-related developmental regulator)	1.15	2.14
DDEF1 (development- and differentiation-enhancing factor 1)	1.12	2.32
FGF7 (fibroblast growth factor 7 [keratinocyte growth factor])	1.05	2.16
KLF8 (Kruppel-like factor 8)	0.83	2.11
MLL2 (myeloid/lymphoid or mixed-lineage leukemia 2)	−1.48	−2.65
TEAD4 (TEA domain family member 4)	−1.38	−2.74
CASP8 (caspase 8, apoptosis-related cysteine protease)	−1.31	−2.19
HLF (hepatic leukemia factor)	−1.29	−2.04
NAB1 (NGFI-A binding protein 1 [EGR1 binding protein 1])	−1.27	−2.35
EPS15 (epidermal growth factor receptor pathway substrate)	−1.24	−3.47
HOXB4 (homeobox B4)	−0.97	−2.05
ZNF175 (zinc finger protein 175)	−0.93	−2.24
Neural factors		
NF2 (neurofibromin 2 [bilateral acoustic neuroma])	1.50	2.53
SEMA4F (sema domain, Ig domain, transmembrane domain, and short cytoplasmic domain [semaphorin] 4F)	1.04	2.20
CHGB (chromogranin B [secretogranin 1])	1.03	2.03
NRG2 (neuregulin 2)	−1.29	−2.90
AB026190 (Kelch motif-containing protein)	−1.29	−2.16
NUP214 (nucleoporin, 214 kDa [CAIN])	−1.19	−2.28
NRP2 (neuropilin 2)	−1.16	−2.81
NOVA2 (neuro-oncological ventral antigen 2)	−1.07	−2.05
GABRA2 (gamma-aminobutyric acid A receptor, alpha 2)	−1.05	−2.47

Continued on facing page

TABLE 1—*Continued*

Gene or protein[a]	SAM score	Fold change
Synthesis, transport, and biochemical pathways		
ALDH6A (methylmalonate-semialdehyde dehydrogenase)	1.79	2.67
UNG (uracil-DNA glycosylase)	1.66	2.60
ST3GALVI (alpha2,3-sialyltransferase)	1.63	3.19
COPB (coatomer protein complex, subunit beta)	1.51	2.34
SPTLC1 (serine palmitoyltransferase, long-chain subunit 1)	1.45	2.21
ATP7B (ATPase, Cu^{2+}-transporting, beta polypeptide) (Wilson's disease)	1.41	2.68
OSBP (oxysterol binding protein)	1.39	2.13
APOB [apolipoprotein B, including Ag(x) antigen]	1.34	2.06
CPT2 (camitine palmitoyltransferase II)	1.33	2.06
GNE (UDP-*N*-acetylglucosamine-2-epimerase/*N*-acetylmannosamine kinase)	1.32	2.26
AP1G2 (adaptor-related protein complex 1, gamma 2 subunit)	1.28	2.17
STX7 (syntaxin 7)	1.23	2.07
AMPD1 (adenosine monophosphate deaminase 1, isoform M)	1.22	2.32
PLTP (phospholipid transfer protein)	1.22	2.28
PCSK5 (proprotein convertase subtilisin/kexin type 5)	1.22	2.05
LOC51170 (retinal shortchain dehydrogenase/reductase)	1.15	2.01
ODC1 (ornithine decarboxylase)	1.10	2.20
NME1 protein [NM23A] expressed in nonmetastatic cells 1)	1.03	2.08
PROSC (proline synthetase cotranscribed [bacterial homolog])	1.03	2.09
CAPN1 (calpain 1 [mu/l] large subunit)	0.99	2.06
ALDH3B1 (aldehyde dehydrogenase 3 family, member B1)	0.97	2.27
SYT5 (synaptotagmin V)	0.95	2.12
ACOX2 (acyl-coenzyme A oxidase 2, branched chain)	0.92	2.05
ATP5C1 (ATP synthase, H^+-transporting, mitochondrial F1 complex, gamma polypeptide 1)	−1.26	−2.17
MGAT1 (mannosyl [alpha-1,3-]-glycoprotein beta-1,2-*N*-acetylglucosaminyltransferase)	−1.25	−2.57
Human glucose transporter pseudogene	−1.24	−2.58
ATP2A2 (ATPase, Ca^{2+} transporting, cardiac muscle, slow twitch 2)	−1.18	−2.29
SRM (spermidine synthase)	−1.18	−2.22
PPIL2 (peptidylprolyl isomerase [cyclophilin]-like 2)	−1.17	−2.67
SDHB (succinate dehydrogenase complex, subunit B, iron sulfur [lp]	−1.09	−2.60
SLC7A5 (solute carrier family 7 [cationic amino acid transporter, y+ system], member 5)	−1.07	−3.19
PYCS (pyrroline-5-carboxylate synthetase [glutamate gamma-semialdehyde synthetase])	−1.01	−2.34
MDH1 (malate dehydrogenase 1, NAD soluble)	−0.98	−2.21
PPIG (peptidyl-prolyl isomerase G [cyclophilin G])	−0.92	−2.68
Miscellaneous		
T1A-2 (lung type-I cell membrane-associated glycoprotein)	1.63	2.62
DREV1 (CGI-81 protein)	1.55	2.45
MADH4 (MAD [mothers against decapentaplegic, *Drosophila*] homolog 4)	1.54	2.36
SDF2L1 (stromal cell-derived factor 2-like 1)	1.50	2.31
DC12 protein	1.49	2.35
SEPN1 (selenoprotein N, 1)	1.44	2.36
NICE-1 protein	1.41	2.58
HGS (hepatocyte growth factor-regulated tyrosine kinase substrate)	1.41	2.33
SEC3 (Sec3-like)	1.38	2.19
POP2 (popeye protein 2)	1.36	2.15
RBM14 (RNA binding motif protein 14)	1.32	2.11
TCTE1L (t-complex associated testis expressed 1-like)	1.27	2.13
SDC3 (syndecan 3 [*N*-syndecan])	1.27	2.08
MAGEF1 protein	1.24	2.23
JTV1 gene	1.21	2.21
LOC51312 (mitochondrial solute carrier)	1.20	2.06
HTPAP protein	1.15	2.10
LOC51578 (adrenal gland protein AD-004)	1.14	2.36
RBMX (RNA binding motif protein, X chromosome)	1.00	2.08
PDYN (prodynorphin)	−1.79	−3.50
ITM2A (integral membrane protein 2A)	−1.78	−3.92
DBY (DEAD/H [Asp-Glu-Ala-Asp/His] box polypeptide)	−1.61	−2.58
TSGA13 (testis specific, 13)	−1.50	−2.72
ZFR (zinc finger RNA binding protein)	−1.43	−2.29
FEM1B (FEM-1 (*C elegans*) homolog b)	−1.42	−2.66
LRMP (lymphoid-restricted membrane protein)	−1.41	−2.49
PELI1 (pellino (*Drosophila*) homolog 1)	−1.39	−3.13
PEAS (testis intracellular mediator protein)	−1.31	−2.50
HBG2 (hemoglobin, gamma G)	−1.29	−2.62
CYLD (cylindromatosis [turban tumor syndrome])	−1.22	−2.45

Continued on following page

TABLE 1—*Continued*

Gene or protein[a]	SAM score	Fold change
WHSC2 (Wolf-Hirschhorn syndrome candidate 2)	−1.17	−2.36
SKD3 (suppressor of potassium transport defect 3)	−1.10	−2.31
PILR(BETA) (paired Ig-like receptor beta)	−0.97	−2.35
COMP (cartilage oligomeric matrix protein [pseudoachondroplasia, epiphyseal dysplasia 1, multiple])	−0.94	−2.36
ESM1 (endothelial cell-specific molecule 1)	−0.90	−2.58
KIAA0105 (Wilms' tumor 1-associating protein)	−0.88	−2.33
HFFs		
Immune and stress response		
Complement component 1, q subcomponent, receptor 1	1.32	2.78
IFITM1 (interferon-induced transmembrane protein 1)	1.16	2.30
CARP (cardiac ankyrin repeat protein)	1.04	2.19
CD24 (CD24 antigen [small cell lung carcinoma cluster 4 antigen])	0.91	2.44
C2 (complement component 2)	0.79	2.16
F2 (coagulation factor II [thrombin])	−1.25	−2.33
IL22R (interleukin-22 receptor)	−1.03	−2.06
Cell adhesion and structure		
KTN1 (kinectin 1 [kinesin receptor])	1.01	2.08
DNCl2 (dynein, cytoplasmic, intermediate polypeptide 2)	0.91	2.13
EPB72 (erythrocyte membrane protein band 7.2 [stomatin])	0.86	2.18
VIL2 (villin 2 [ezrin])	0.79	2.01
KIF5B (kinesin family member 5B)	−1.11	−2.14
Signal transduction: receptors, kinases/phosphatases, G proteins		
VRK2 (vaccinia virus-related kinase 2)	1.48	2.51
S100A13 (S100 calcium-binding protein A13)	1.29	2.40
SHB (SHB adaptor protein [a Src homology 2 protein])	1.28	2.24
DAPK3 (death-associated protein kinase 3)	1.03	2.34
PPP1R2 (protein phosphatase 1, regulatory [inhibitor] subunit 2)	0.84	2.02
EFNB2 (ephrin-B2)	0.83	2.10
STC2 (stanniocalcin 2)	0.81	2.17
SSI-1 (JAK binding protein)	−1.39	−2.38
ADORA2B (adenosine A2b receptor)	−1.29	−2.41
HTR2A (5-hydroxytryptamine [serotonin] receptor 2A)	−1.12	−2.51
DLG1 (discs large [*Drosophila*] homolog 1)	−0.76	−2.40
Replication, transcription, translation, degradation machinery, protein modification		
FBXO25 (F-box only protein 25)	1.00	2.29
HNRPH3 (heterogeneous nuclear ribonucleoprotein H3 [2H9])	0.97	2.19
RPS24 (ribosomal protein S24)	0.94	2.23
ADAMTS6 (a disintegrin-like and metalloprotease [reprolysin type] with thrombospondin type 1 motif)	2.00	2.05
RPS5 (ribosomal protein S5)	−1.62	−2.11
POLR2D (polymerase [RNA] II [DNA directed] polypeptide D)	−1.19	−2.66
Cell cycle, development, apoptosis, transcription factors		
Spinocerebellar ataxia 2 (olivopontocerebellar ataxia 2, autosomal dominant, ataxin 2)	0.90	2.12
LATS2 (LATS (large tumor suppressor, [*Drosophila*] homolog 2)	0.88	2.01
JUNB (jun B proto-oncogene)	0.83	2.02
ZNF38 (zinc finger protein 38 [KOX 25])	0.82	2.21
PLXNB2 (plexin B2)	0.82	2.02
GTF2F2 (general transcription factor IIF, polypeptide 2 [30-kDa subunit])	−1.22	−2.43
BIRC2 (baculoviral IAP repeat-containing 2)	−1.09	−2.11
CHES1 (checkpoint suppressor 1)	−1.09	−2.12
Synthesis, transport, and biochemical pathways		
CPB2 (carboxypeptidase B2 [plasma, carboxypeptidase U])	1.19	2.33
SCLY (putative selenocysteine lyase)	1.17	2.53
SRRM2 (serine/arginine repetitive matrix 2)	1.01	2.34
QDPR (quinoid dihydropteridine reductase)	1.00	2.07
GLRX (glutaredoxin [thioltransferase])	0.88	2.02
LOC51635 (CGI-86 protein)	0.83	2.07
FDPS (farnesyl diphosphate synthase [farnesyl pyrophosphate synthetase, dimethylallyltranstransferase, geranyltranstransferase])	0.69	2.09

Continued on facing page

TABLE 1—*Continued*

Gene or protein[a]	SAM score	Fold change
CA1 (carbonic anhydrase l)	−1.19	−2.05
ABCC3 (ATP-binding cassette, subfamily C [CFTR/MRP], member 3)	−1.10	−2.25
MPI (mannose phosphate isomerase)	−1.00	−2.33
Miscellaneous		
MEA (male-enhanced antigen)	1.30	2.69
PRDX3 (peroxiredoxin 3)	1.08	2.28
TEM5 (tumor endothelial marker 5 precursor)	0.84	2.20
UCP2 (uncoupling protein 2 [mitochondrial, proton carrier])	0.77	2.15
DKK3 (Dickkopf (*Xenopus laevis*) homolog 3)	−1.02	−2.03

[a] Human expressed sequence tags and genes with no known function are not included but can be found at http://cmgm.stanford.edu/~jjones. Items in boldface are similarly regulated in human cells by other herpesvirus infections.

replicates more slowly than pOka in skin implants, the samples were harvested from SCIDhu mice at late times after infection, when vOka and pOka titers are similar.

Effects of VZV on gene transcription in T cells. To generate the list of host cell genes that were regulated significantly in VZV-infected T cells, the one-class analyses of seven T-cell arrays were further corrected by eliminating genes that showed variance by two-class analyses, as noted above. Transcription of a total of 373 genes was altered significantly. Of these, 218 genes were up-regulated and 155 genes were down-regulated in VZV-infected T cells at 48 h after infection (Table 1). The classifications of genes that were affected included those involved in immune and stress responses, cell adhesion, cell structure, signal transduction, cell cycle, apoptosis, and other cell functions. The interferon response was markedly induced, as typified by the increase of transcripts such as those for RNA-specific adenosine deaminase (ADAR) and myxovirus resistance 2 (MX2). The ability of the virus to co-opt the basic host cell machinery is also evident from the altered transcription of many genes involved in synthesis, transport, replication, transcription, and translation.

Effects of VZV on gene transcription in fibroblasts. One-class response analyses of VZV-infected HFFs showed that expression profiles of 91 genes were altered, with an increase in transcription of 63 genes and a decrease in transcription of 28 genes (Table 1). Fewer significantly regulated genes were detected in HFFs than in T cells, but this result was expected because seven experiments were done with VZV-infected T cells compared to four with HFF specimens. Under the stringent validation rules that were used, statistical confirmation of a significant transcriptional change is achieved more often as the data set is expanded to include more separately performed microarray experiments. Though not a major target of VZV pathogenesis in vivo, fibroblasts are readily infectible, and HFFs are used commonly to investigate VZV replication. An interferon response in HFFs as well as T cells was documented. The transcription of signal transducers and activators of transcription (STAT)-induced STAT inhibitor-1 (SSI-1), which is also referred to as suppressor of cytokine signaling 1 (SOCS-1), in fibroblasts was decreased, allowing for increased interferon-induced transcriptional activation. As in VZV-infected T cells, many transcriptionally altered genes were those of the basic cell machinery, including two genes that encode important microtubule-associated motor proteins, kinectin and dynein, which may have important functions in the transport of herpesvirus virions.

Effects of VZV on gene transcription in skin. One-class response analyses showed that 129 genes in VZV-infected skin xenografts had altered expression profiles, including 64 genes that were up-regulated and 65 genes that were down-regulated, compared to profiles in uninfected xenografts (Table 2). These one-class response analyses were based on data from seven microarrays, and results were corrected for variance by two-class response comparisons. Although T-cell and skin analyses were based on equal numbers of microarrays, fewer significantly regulated genes were returned in the analysis of skin specimens. The rigorous criteria for identifying altered transcription patterns were essential in these experiments because skin implants contain subpopulations of differentiated cells, and even those harvested at 28 days after VZV inoculation contain cells that remain uninfected (19). These factors were expected to reduce the number of host cell genes that were detected as being significantly regulated genes. The response of skin cells to VZV infection was characterized by most transcriptional changes being in basic cell machinery genes. Of note, the transcription of a number of genes involved in cell structure, such as that encoding keratin 5, was also altered. Keratin 5 is a type II keratin responsible for the structural integrity of the epidermis, which appears to be the first site of VZV replication in skin tissue (C.-C. Ku, unpublished data).

Comparison of transcriptional changes among host cell types infected with VZV. Two-class response analyses were also used to compare transcriptional responses between cell types. These comparisons yielded fewer genes that were found to be significantly regulated because, as the number of microarrays in each data set increases, it becomes less likely for a particular gene to pass the strict filtering criteria on >70% of the microarrays (Table 3). Nevertheless, differences in gene regulation that emerge from such comparisons are of interest for VZV pathogenesis. The analysis identified genes that had a twofold difference in regulation between the cell types and that passed the statistical requirements of the SAM program (see website). In most cases, a particular gene was regulated significantly in one cell type while displaying no difference from the

TABLE 2. Significantly regulated genes in VZV-infected SCIDhu human skin implants

Gene or protein[a]	SAM score	Fold change
Immune and stress response		
LY6E (lymphocyte antigen 6 complex, locus E)	3.35	0.74
G1P3 (alpha interferon-inducible protein [clone IFI-6-16])	3.22	0.68
CD68 antigen	2.32	1.02
PTAFR (platelet-activating factor receptor)	1.92	0.75
DF (D component of complement [adipsin] interleukin-24)	−3.22	−0.90
	−2.89	−0.81
Cell adhesion and structure		
MUC6 (mucin 6, gastric)	2.27	1.02
ARPC4 (actin-related protein 2/3 complex, subunit 4 [20 kDa])	4.14	0.71
COL1A1 (collagen, type I, alpha 1)	−2.57	−1.64
Myosin, light polypeptide 9	−2.11	−1.15
Keratin 5	−1.90	−2.20
Keratin 5	−1.82	−1.96
Keratin 5	−1.74	−1.36
Signal transduction: receptors, kinases/phosphatases, G proteins		
CACNA1D (calcium channel, voltage dependent, L type, alpha 1D subunit)	2.60	0.61
RGS7 (regulator of G-protein signaling 7)	2.50	0.88
PIK4CB (phosphatidylinositol 4-kinase, catalytic, beta polypeptide)	2.36	0.52
TNFRSF1B (tumor necrosis factor receptor superfamily, member 1B)	2.19	0.71
RGS6 (regulator of G-protein signaling 6)	2.06	0.70
PRKAG2 (protein kinase, AMP-activated, gamma 2 noncatalytic subunit)	2.06	0.61
ASGR1 (asialoglycoprotein receptor)	2.02	0.75
PRKCE (protein kinase C, epsilon)	1.96	0.69
Protein tyrosine phosphatase, nonreceptor type 13 (APO-1/CD95 [Fas]-associated phosphatase)	−2.95	−0.95
Replication, transcription, translation, Degradation machinery, protein modification		
Cathepsin F	3.40	0.76
Cathepsin K (pycnodysostosis)	2.69	0.78
SSR1 (signal sequence receptor, alpha)	2.59	0.83
PTRF polymerase I and transcript release factor	1.95	0.72
Topoisomerase (DNA) III beta	1.94	0.55
EEF1A1 (eukaryotic translation elongation factor 1 alpha 1)	−5.21	−3.01
EEF1G (eukaryotic translation elongation factor 1 gamma)	−3.94	−2.29
RPL12 (ribosomal protein L12)	−3.46	−1.64
RPL9 (ribosomal protein L9)	−3.27	−1.61
RPS8 (ribosomal protein S8)	−3.20	−3.40
RPS25 (ribosomal protein S25)	−3.07	−1.32
RPL6 (ribosomal protein L6)	−2.88	−1.39
RPL29 (ribosomal protein L29)	−2.09	−1.19
RPL23A (ribosomal protein L23a)	−2.09	−1.47
RPL35 (ribosomal protein L35)	−2.02	−1.40
EEF2 (eukaryotic translation elongation factor 2)	−1.98	−0.95
RPL23 (ribosomal protein L23)	−1.89	−1.41
RPL18A (ribosomal protein L18a)	−1.78	−1.29
RPL35A (ribosomal protein L35a)	−1.69	−1.15
RPS15 (ribosomal protein S15)	−1.67	−1.56
RPL41 (ribosomal protein L41)	−1.67	−1.64
RPS5 (ribosomal protein S5)	−1.45	−1.56
RPS28 (ribosomal protein S28)	−1.22	−1.10
RFC3 (replication factor C [activator 1] 3 [38 kDa])	−2.14	−0.58
Cell cycle, development, apoptosis, transcription factors		
CEP2 (Cdc42 effector protein 2)	3.35	0.86
GAS2 (growth arrest specific 2)	3.11	1.16
ELK1 (member of ETS oncogene family)	2.54	1.12
ERBB3 (v-erb-b2 erythroblastic leukemia viral oncogene homolog 3)	2.52	1.04
ATF6 (activating transcription factor 6)	2.41	0.55
GTF3C1 (general transcription factor IIIC polypeptide 1, alpha subunit)	2.25	0.53
TFAP2A (transcription factor AP-2 alpha [activating enhancer binding protein 2 alpha])	1.83	0.55
HIR (histone cell cycle regulation defective homolog A [*S. cerevisiae*])	1.82	0.64
MYC (v-myc myelocytomatosis viral oncogene homolog [avian])	1.79	0.64

Continued on facing page

TABLE 2—*Continued*

Gene or protein[a]	SAM score	Fold change
GADD45A (growth arrest and DNA damage inducible, alpha)	−1.83	−0.99
Synthesis, transport, and biochemical pathways		
ANPEP (alanyl [membrane] [aminopeptidase N, CD13, p150])	3.64	0.67
BGN (biglycan)	3.17	1.05
DNMT2 (DNA [cytosine-5-]-methyltransferase 2)	2.65	2.02
PMM2 (phosphomannomutase 2)	2.56	0.81
INPP5D (inositol polyphosphate-5-phosphatase, 145 kDa)	2.50	0.54
DNMT2 (DNA [cytosine-5-]-methyltransferase 2)	2.48	0.80
PDE6D (phosphodiesterase 6D, cGMP-specific, rod, delta)	2.45	0.79
B4GALT3 (UDP-Gal:betaGlcNAc beta 1,4-galactosyltransferase, polypeptide 3)	2.42	0.78
HAAO (3-hydroxyanthranilate 3,4-dioxygenase)	2.36	0.71
TRN2 (karyopherin beta 2b, transportin)	2.27	0.67
MLC1SA (myosin light chain 1 slow a)	1.66	0.87
NDUFS2 (NADH dehydrogenase [ubiquinone] Fe-S protein2 (49 kDa) [NADH-coenzyme Q reductase])	1.79	0.66
PPIC (peptidylprolyl isomerase C [cyclophilin C])	−5.87	−1.45
PPIB (peptidylprolyl isomerase B [cyclophilin B])	−4.57	−0.85
ARF1 (ADP-ribosylation factor 1)	−2.35	−0.91
PHGDH (phosphoglycerate dehydrogenase)	−2.21	−1.61
CHI3L1 (chitinase 3-like 1 [cartilage glycoprotein-39])	−1.48	−1.02
NDUFA10 (NADH dehydrogenase [ubiquinone] 1 alpha subcomplex 10)	−1.94	−0.70
DDT (D-dopachrome tautomerase)	−2.04	−0.57
Miscellaneous		
CST1 (cystatin SN)	3.65	0.86
NCSTN (nicastrin)	3.55	0.75
CHRNE (cholinergic receptor, nicotinic, epsilon polypeptide)	3.46	0.67
C21 orf25 (chromosome 21 ORF 25)	3.14	0.73
FVT1 (follicular lymphoma variant translocation 1)	3.09	1.39
EMD (emiren)	2.84	0.71
RBM3 (RNA binding motif protein 3)	2.61	0.59
ZNF297 (zinc finger protein 297)	2.53	0.69
AP1S1 (adaptor-related protein complex 1, sigma 1 subunit)	2.52	0.76
DPEP1 (dipeptidase 1 [renal])	2.48	0.53
DRIL 1 (dead ringer-like 1)	2.46	0.80
MAFG (v-maf musculoaponeurotic fibrosarcoma oncogene homolog)	2.45	0.92
DLX4 (distal-less homeobox 4)	2.30	0.71
ZFP36 (zinc finger protein 36, C3H type, homolog [mouse])	2.09	0.81
GRAP2 (GRB2-related adaptor protein 2)	2.11	0.69
AP3B1 (adaptor-related protein complex 3, b1)	2.05	0.58
PEA15 (phosphoprotein enriched in astrocytes 15)	1.97	0.78
MAZ (MYC-associated zinc finger protein)	1.96	0.62
CAT56 protein	1.96	0.52
Small proline-rich protein SPRK	1.75	0.66
KLK3 (kallikrein 3)	−2.65	−2.35
DSP (desmoplakin [DPI, DPII])	−2.47	−1.34
SMARCD2 (SWI/SNF related)	−2.20	−1.84
Progastricsin (pepsinogen C)	−3.25	−0.55
Homo sapiens thymosin, beta 4	−2.80	−1.77
NME2 nonmetastatic cells 2 protein (NM23B)	−2.74	−0.70
MLL2 (myeloid/lymphoid or mixed-lineage leukemia 2)	−2.06	−0.80

[a] Human expressed sequence tags and genes with no known function are not included in this table but can be found at http://cmgm.stanford.edu/~jjones. Items in boldface in this table are similarly regulated in human cells by other herpesvirus infections.

uninfected control (not significantly regulated) in the other cell type.

VZV infection of each of the cell types examined had some common effects, including the induction of an interferon response and alteration of the basic cell machinery genes. However, as each differentiated cell type contains a unique transcriptional repertoire, the virus must adapt to each environment accordingly. Therefore, changes in the regulation of some transcripts are likely to be observed only in one cell type. Among differences of interest, transcription of the gene encoding caspase 8, which is a major regulator of apoptotic pathways, was down-regulated in T cells but remained unchanged in HFFs and skin. This difference could reflect the need to increase the longevity of T cells during cell-associated viremia in order for VZV to spread from the site of mucosal inoculation to cutaneous sites of replication. The relative

TABLE 3. Comparison of gene regulation in VZV-infected T cells, HFFs, and skin

Functional category	Proteins encoded by genes for which:				
	T cells > HFF	HFF > T cells	Skin > T cells	T cells > skin	HFF > skin	Skin > HFF
Immune and stress response	FCER1G, CD32, granulysin, ADAR, CD49C, interleukin-17B, MIP-1α, ILF1, regulatory factor X, 2 (influences HLA class II expression), MX2, eotaxin, ILF3, MIG1, MHC2TA	MIG2, MICA, CD47, MHC-I region ORF P5-1, HLA-C, IFITM1, SCYB10, CD3D, CLPP, fractalkine, MX1, PRKR, WSX-1, CISH, AIFI	CD68	Complement component 7, RAE1 homolog, glycophorin B		
Cell adhesion and cell structure	collagen type VI alpha2	SPTA1, ICAM1, ITGAM	Biglycan	SELIL, synuclein alpha, desmuslin		APPBP2
Signal transduction	Cannabinoid receptor, TOSO, TNFSF13, FAF1, MAPK4, SSI-3 (STAT-induced STAT inhibitor 3)	VRK2, PIK3CA, PPP2R1A, PPP1R2, PRKAR1B, PMI, DDR1, TNFRSF14	MAP2K4, dual-specificity phosphatase 5	PPP2CA, Rho guanine exchange factor 16, PPIB, STAT6		PRKAG2, guanylate kinase 1
Replication, transcription, etc.	POLR2D	polybromo 1, PSMB3, cathepsin L, cathepsin D		Ubiquitin specific protease 4, RNase 6, TAF12, ZNF74, SMARCD2	Ribosomal proteins L21 and L10, SRRM2	SFRS2IP
Cell cycle, development, etc.	Fibroblast growth factor 2, colony-stimulating factor 2 receptor beta, fibroblast growth factor 1	caspase 8, TGFB3, EPS15, JUNB, TGFBI, SCA2, 101F6, MMD	TRIP11, FVT1, WHSC1	FGF7, TES, GAP43, PMP22, ETS2		FVT1, Cdc42 effector protein 2, insulin-like growth factor 2
Synthesis, transport, biochemical pathways	PRG1	LSS, prodynorphin	Asialoglycoprotein receptor 1, PYCS	GNE, IHPK1, ALAS2, FDPS, ODC1, PLP2	Peptidylprolyl isomerase B, CYP19, aquaporin 5, UQCRB	Arginase

down-regulation of MHC-I polypeptide-related sequence A (MICA), which is a natural killer cell-activating ligand, could reflect a cell type-specific mechanism to avoid recognition of VZV-infected T cells by NK cells.

Confirmation of microarray findings. Though SAM analysis of the microarray data revealed little variance among arrays of the same cell type, real-time RT-PCR was used to verify the accuracy of the transcriptional changes in selected genes, as detected by microarray, of VZV-infected T cells. Three genes were chosen for analysis, two that were up-regulated and one that was down-regulated (Table 4); β-globin was used as a control. Only data that could be compared to a valid standard curve were used. Although the absolute RT-PCR values are not identical to the microarray data due to intrinsic differences between the techniques, the RT-PCR data show the same relative regulation of transcription and therefore corroborate the microarray data. The transcription of the β-globin gene in all experiments was unaltered. The finding that caspase 8 was down-regulated in T cells but not HFFs was also confirmed by RT-PCR. Additionally, the up-regulation of one gene, that encoding gp96, was further confirmed at the protein level by Western blotting (Fig. 2).

DISCUSSION

This work represents the first global analysis of the transcriptional response of host cells to VZV infection. The experiments were designed to assess patterns of gene expression in primary T cells and skin xenografts, which are the cell types targeted during the pathogenesis of primary VZV infection, and in fibroblasts, which are a common laboratory cell line used for propagating VZV. To ensure the accurate identification of genes whose regulation was significantly altered in response to VZV infection, the array data were scrutinized and stringently filtered, and the SAM program was utilized to determine statistical significance. With these methods for assay validation and statistical verification, the use of the human cDNA arrays permitted the detection of altered expression of 373 T-cell genes, 91 fibroblast genes, and 129 genes in skin xenografts that were associated with VZV infection (Tables 1 and 2).

This study begins to define genes whose regulation is altered specifically in response to VZV infection and can be used to identify genes whose regulation is altered generally in response to herpesvirus infection. Nevertheless, comparisons among microarray datasets must take into account the similarities or differences of experimental conditions, particularly of the target cell type. Both human cytomegalovirus (HCMV) and herpes simplex virus type 1 (HSV-1) infections of human fibroblasts have also been studied by microarray. Assessment of the transcriptional response of fibroblasts to HCMV infection revealed many of the same effects as our analysis of VZV-infected fibroblasts (10). Some commonly regulated genes included those encoding CD38, regulator of G-protein signaling 6, and mitogen-activated protein kinase 8-interacting protein 2. The response of fibroblasts to inactivated, replication-deficient, and wild-type HSV-1 strains in fibroblasts was also associated with many of the same transcriptional alterations, such as up-regulation of interferon-induced transmembrane protein 1, which is involved in the transduction of antiprolif-

TABLE 4. Confirmation of microarray findings by real time RT-PCR

Gene product	T-cell fold change by:	
	Microarray	RT-PCR
MX2 (myxovirus [influenza virus] resistance 2, homolog of murine)	2.36	10.57
ADAR (RNA specific)	2.04	6.46
CASP8 (caspase 8, apoptosis-related cysteine protease)	−2.19	−1.69

erative and homotypic adhesion signals (20). It is likely that many common signaling pathways will be altered by herpesviruses and that the responses of the host cell to these viruses will be similar. However, the HSV-1 study also demonstrated that two of the most prominent interferon response genes, those encoding ADAR and MX2, were induced by inactivated and replication-deficient strains but not by infectious HSV-1, suggesting that wild-type HSV-1 has a mechanism to block such induction. Both of these two genes were up-regulated significantly in VZV-infected T cells, indicating that HSV-1 may have evolved an immunoevasion mechanism that VZV lacks.

Interestingly, the transcription of the gene encoding caspase 8, a major regulator of both ligand-mediated and mitochondrion-mediated apoptosis, was down-regulated in VZV-infected T cells, as determined by microarray and as confirmed by RT-PCR, while a microarray study of human herpesvirus 6 (HHV-6) infection of an immortalized T-cell line demonstrated an increase in caspase 8 mRNA (17). This difference could simply reflect the use of primary versus immortalized T cells, or it may represent a difference in VZV and HHV-6 pathogenesis. Since VZV-infected T cells appear to transport virus to the skin, where infectious lesions form, repression of apoptosis in VZV-infected T cells is likely to be important to the person-to-person spread of virus. In a response that is likely to benefit the host, VZV infection of T cells was associated with increased transcription and translation of the gene encoding gp96 (tumor rejection antigen 1 or grp94). Transcription of the gp96 gene in Caco-2 cells infected with rotavirus was also increased (13). gp96 is a prototypical heat shock protein that resides normally in the lumen of the endoplasmic reticulum but that is transported to the cell surface under stress conditions (3). In addition, gp96 binds to CD91 on antigen-presenting cells and undergoes receptor-mediated endocytosis (9); gp96 binding induces dendritic-cell maturation and facilitates transfer of gp96-associated peptides from the extracellular compartment to MHC-I molecules by both direct endocytosis of gp96 and by phagocytosis of apoptotic debris containing the protein (31). This molecule may be important in the cross-presentation of viral antigen (21), especially when the virus is able to interfere with MHC antigen presentation, as VZV does (1, 2).

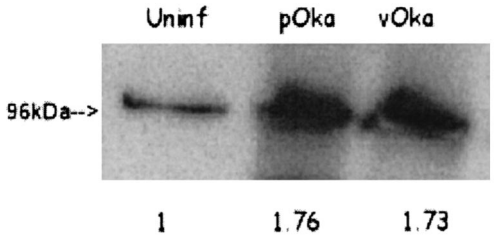

FIG. 2. Expression of gp96 in VZV-infected T cells. Total cell lysate from infected or mock-infected T cells was probed with a polyclonal antibody against gp96. A single band was detected at approximately 96 kDa. The increase of expression relative to the uninfected (uninf) control is indicated by the values below each lane; the values were normalized to the total amount of protein added to the gel.

Microarrays have not been used previously to examine skin cells after viral infection in vivo, but effects of human papillomaviruses (HPV) on cultured keratinocytes have been evaluated (11, 27). Of interest, desmoplakin, which functions to stabilize desmosomes, the main adhesive junctions in epithelial tissues, was down-regulated in VZV-infected skin and in keratinocytes infected with HPV type 31 (HPV-31). The levels of transcription of the 3-phosphoglycerate dehydrogenase gene were decreased, whereas those of the oncogenic maf gene were increased, similarly in response to HPV-11 and VZV. The regulation of these genes may reflect common mechanisms of host cell manipulation used by viruses that replicate in and are transmitted from mucocutaneous sites.

Comparative microarray analysis of VZV-infected T cells, fibroblasts, and skin demonstrated many differences in the response phenotype of host cell genes in each cell type. The distinctive responses can be expected to influence or reflect mechanisms of VZV pathogenesis in differentiated cells, as well as how each cell type attempts to control replication of the virus and alert the immune system to its presence. Since the normal transcriptional patterns of differentiated cells vary, the virus must respond to each of these environments in a unique fashion. For instance, our experiments indicate that VZV infection caused a marked decrease in keratin 5 mRNA. This effect probably allows the virus to cause the ballooning degeneration and disruption of keratinocyte integrity observed by histological examination of cutaneous VZV lesions. Expression of keratin 5 is unique to skin cells and would therefore not likely be altered by VZV infection of T cells. However, differences in the responses of other genes to VZV may reflect cell type-specific effects of the virus on their transcription. For example, VZV appears to have the capacity to block apoptosis in a cell type-specific manner. The transcription of the gene encoding caspase 8, a major regulator of both ligand-mediated and mitochondrion-mediated apoptosis, in VZV-infected T cells was down-regulated, while its transcription in VZV-infected fibroblasts and skin remained unchanged. Changes in transcription of genes involved in signal transduction also differed between T cells and skin. Levels of transcription of genes encoding the mitogen-activated kinase MAP2K4 and the dual-specificity phosphatase 5 in T cells were higher than those in skin, while levels of transcription of genes, such as those encoding Rho guanine exchange factor 16 and STAT-6, in VZV-infected T cells were lower than those in skin.

One potential application of microarray analysis of virus-host cell interactions is to characterize differences among virus strains. Our experiments identified no significant differences between the host gene response to infection with pOka and the response to vOka in T cells, HFFs, or skin. The data set for the two-class analysis of pOka versus vOka in T cells was robust, since it consisted of three pOka and four vOka arrays, and the

HFF data set included two pOka and two vOka arrays. Failure to observe differences between pOka and vOka is consistent with the fact that the growth kinetics of pOka and vOka in T cells and in HFFs in vitro and at late times after infection in skin in vivo are indistinguishable. The fact that the changes induced by infection of target cells with pOka and vOka were similar suggests that the attenuated phenotype of the vaccine virus is not due to a few major alterations in its effects on host cell gene expression but rather results from a combination of more subtle changes. As the replication kinetics of vOka in skin implants in SCIDhu mice have been shown to be delayed, a significant difference between pOka and vOka infection might be observed at earlier time points (19).

The use of microarrays to demonstrate differences in effects on host cell genes in primary, biologically relevant cell types provides background information for experiments to link these various response phenotypes with mechanisms of VZV pathogenesis that are important for the natural course of human infection.

ACKNOWLEDGMENTS

This work was supported by a National Science Foundation graduate fellowship to Jeremy O. Jones and by a grant from the National Institute of Allergy and Infectious Diseases, AI20459, to A.M.A.

We thank Jason Lih and Ira Blader for assistance with the microarray experiments and the David Schneider laboratory for assistance with the RT-PCR experiments.

REFERENCES

1. **Abendroth, A., B. Slobedman, E. Lee, E. Mellins, M. Wallace, and A. M. Arvin.** 2000. Modulation of major histocompatibility class II protein expression by varicella-zoster virus. J. Virol. **74:**1900–1907.
2. **Abendroth, A., I. Lin, B. Slobedman, H. Ploegh, and A. M. Arvin.** 2001. Varicella-zoster virus retains major histocompatibility complex class I proteins in the Golgi compartment of infected cells. J. Virol. **75:**4878–4888.
3. **Altmeyer, A., R. G. Maki, A. M. Feldweg, M. Heike, V. P. Protopopov, S. K. Masur, and P. K. Srivastava.** 1996. Tumor-specific cell surface expression of the-KDEL containing, endoplasmic reticular heat shock protein gp96. Int. J. Cancer **69:**340–349.
4. **Annunziato, P. A., and A. A. Gershon.** 2000. Primary immunization against varicella, p. 460–476. *In* A. Arvin and A. Gershon (ed.), Varicella-zoster virus: virology and clinical management. Cambridge University Press, Cambridge, United Kingdom.
5. **Argaw, T., J. I. Cohen, M. Klutch, K. Lekstrom, T. Yoshikawa, Y. Asano, and P. R. Krause.** 2000. Nucleotide sequences that distinguish Oka vaccine from parental Oka and other varicella-zoster virus isolates. J. Infect. Dis. **181:** 1153–1157.
6. **Arvin, A.** 1998. Varicella-zoster virus: virologic and immunologic aspects of persistent infection, p. 183–208. *In* R. Ahmed and I. Chen (ed.), Persistent viral infections. John Wiley & Sons Ltd., New York, N.Y.
7. **Arvin, A. M.** 2001. Varicella vaccine: genesis, efficacy, and attenuation. Virology **284:**153–158.
8. **Arvin, A. M.** 2001. Varicella-zoster virus, p. 2731–2768. *In* D. N. Knipe and P. M. Howley (ed.), Fields virology, 4th ed., vol. 2. Lippincott-Raven Publishers, Philadelphia, Pa.
9. **Binder, R. J., D. K. Han, and P. K. Srivastava.** 2000. CD91: a receptor for heat shock protein gp96. Nat. Immunol. **1:**151–155.
10. **Browne, E. P., B. Wing, D. Coleman, and T. Shenk.** 2001. Altered cellular mRNA levels in human cytomegalovirus-infected fibroblasts: viral block to the accumulation of antiviral mRNAs. J. Virol. **75:**12319–12330.
11. **Chang, Y. E., and L. A. Laimins.** 2000. Microarray analysis identifies interferon-inducible genes and Stat-1 as major transcriptional targets of human papillomavirus type 31. J. Virol. **74:**4174–4182.
12. **Cohen, J. I., and S. E. Straus.** 2001. Varicella-zoster virus and its replication, p. 2707–2730. *In* D. N. Knipe and P. M. Howley (ed.), Fields virology, 4th ed., vol. 2. Lippincott-Raven Publishers, Philadelphia, Pa.
13. **Cuadras, M. A., D. A. Feigelstock, S. An, and H. B. Greenberg.** 2002. Gene expression pattern in Caco-2 cells following rotavirus infection. J. Virol. **76:**4467–4482.
14. **Gomi, Y., T. Imagawa, M. Takahashi, and K. Yamanishi.** 2000. Oka varicella vaccine is distinguishable from its parental virus in DNA sequence of open reading frame 62 and its transactivation activity. J. Med. Virol. **61:**497–503.
15. **Lim, S. M., S. W. Song, S. L. Kim, Y. J. Jang, K. H. Kim, and H. J. Kim.** 2000. Comparison between of the attenuated BR-Oka and the wild type strain of varicella zoster virus (VZV) on the DNA level. Arch. Pharm. Res. **23:**418–423.
16. **Mallory, S., M. Sommer, and A. M. Arvin.** 1997. Mutational analysis of the role of glycoprotein I in varicella-zoster virus replication and its effects on glycoprotein E conformation and trafficking. J. Virol. **71:**8279–8288.
17. **Mayne, M., C. Cheadle, S. S. Soldan, C. Cermelli, Y. Yamano, N. Akhyani, J. E. Nagel, D. D. Taub, K. G. Becker, and S. Jacobson.** 2001. Gene expression profile of herpesvirus-infected T cells obtained using immunomicroarrays: induction of proinflammatory mechanisms. J. Virol. **75:**11641–11650.
18. **Moffat, J. F., M. D. Stein, H. Kaneshima, and A. M. Arvin.** 1995. Tropism of varicella-zoster virus for human $CD4^+$ and $CD8^+$ T lymphocytes and epidermal cells in SCID-hu mice. J. Virol. **69:**5236–5242.
19. **Moffat, J. F., L. Zerboni, P. R. Kinchington, C. Grose, H. Kaneshima, and A. M. Arvin.** 1998. Attenuation of the vaccine Oka strain of varicella-zoster virus and role of glycoprotein C in alphaherpesvirus virulence demonstrated in the SCID-hu mouse. J. Virol. **72:**965–974.
20. **Mossman, K. L., P. F. Macgregor, J. J. Rozmus, A. B. Goryachev, A. M. Edwards, and J. R. Smiley.** 2001. Herpes simplex virus triggers and then disarms a host antiviral response. J. Virol. **75:**750–758.
21. **Nieland, T. J., M. C. Tan, M. Monne-van Muijen, F. Koning, A. M. Kruisbeek, and G. M. van Bleek.** 1996. Isolation of an immunodominant viral peptide that is endogenously bound to the stress protein GP96/GRP94. Proc. Natl. Acad. Sci. USA **93:**6135–6139.
22. **Ruyechan, W. T., and J. Hay (ed.).** 2000. VZV replication in varicella zoster virus: virology and clinical management. Cambridge University Press, Cambridge, United Kingdom.
23. **Schena, M., D. Shalon, R. W. Davis, and P. O. Brown.** 1995. Quantitative monitoring of gene expression patterns with a complementary DNA microarray. Science **270:**467–470.
24. **Sherlock, G., T. Hernandez-Boussard, A. Kasarskis, G. Binkley, J. C. Matese, S. S. Dwight, M. Kaloper, S. Weng, H. Jin, C. A. Ball, M. B. Eisen, P. T. Spellman, P. O. Brown, D. Botstein, and J. M. Cherry.** 2001. The Stanford Microarray Database. Nucleic Acids Res. **29:**152–155.
25. **Sommer, M. H., E. Zagha, O. K. Serrano, C. C. Ku, L. Zerboni, A. Baiker, R. Santos, M. Spengler, J. Lynch, C. Grose, W. Ruyechan, J. Hay, and A. M. Arvin.** 2001. Mutational analysis of the repeated open reading frames, ORFs 63 and 70 and ORFs 64 and 69, of varicella-zoster virus. J. Virol. **75:**8224–8239.
26. **Takahashi, M., T. Otsuka, Y. Okuno, Y. Asano, and T. Yazaki.** 1974. Live vaccine used to prevent the spread of varicella in children in hospital. Lancet **ii:**1288–1290.
27. **Thomas, J. T., S. T. Oh, S. S. Terhune, and L. A. Laimins.** 2001. Cellular changes induced by low-risk human papillomavirus type 11 in keratinocytes that stably maintain viral episomes. J. Virol. **75:**7564–7571.
28. **Tusher, V. G., R. Tibshirani, and G. Chu.** 2001. Significance analysis of microarrays applied to the ionizing radiation response. Proc. Natl. Acad. Sci. USA **98:**5116–5121.
29. **White, C. J.** 1997. Varicella-zoster virus vaccine. Clin. Infect. Dis. **24**:753–763.
30. **Zerboni, L., M. Sommer, C. F. Ware, and A. M. Arvin.** 2000. Varicella-zoster virus infection of a human CD4-positive T-cell line. Virology **270:**278–285.
31. **Zheng, H., J. Dai, D. Stoilova, and Z. Li.** 2001. Cell surface targeting of heat shock protein gp96 induces dendritic cell maturation and antitumor immunity. J. Immunol. **167:**6731–6735.